THE JOURNAL OF PHYSICAL CHEMISTRY A LETTERS

2008, *112,* 1677−1682
Published on Web 02/06/2008

Release of Nitric Oxide and Iodine to the Atmosphere from the Freezing of Sea-Salt Aerosol Components

Paul O'Driscoll,[†] Nicholas Minogue,[†] Norimichi Takenaka,[‡] and John Sodeau*,[†]

Department of Chemistry, University College Cork, Ireland, and Graduate School of Engineering, Osaka Prefecture University, 1-1 Gakuen-cho, Sakai City, Osaka 599-8531, Japan

Received: October 30, 2007; In Final Form: January 2, 2008

The known room-temperature, solution-phase reaction between nitrite ions and iodide ions, which occurs in acidic conditions (pH < 5.5), is shown to be accelerated when neutral aqueous solutions are frozen. The reaction is proposed to occur in liquid "micropockets" within the ice structure at temperatures between the freezing point and the eutectic temperature. The products, nitric oxide and molecular iodine, are known to play significant roles in atmospheric compositional change, and therefore, the results obtained here, which are not dependent on acidification, may impact on observed snowpack chemistry. Investigation of the effect of oxygen on the chemical processing indicates that a chain reaction mechanism is operative.

Introduction

The discovery over Antarctica of a seasonally variable phenomenon resulting in high ozone depletion was originally made by Farman et al.[1] and later related to heterogeneous processing catalyzed by low-temperature particulate matter.[2] The observation has led to a general search for physical phenomena that can perturb the chemistry in the Earth's cryosphere. Subsequently, the discovery of ozone depletion events (ODE) within the polar marine boundary layer in the mid-1980s[3−5] has given further impetus to both field and laboratory studies in which halogen compounds that can be photolyzed by the sun are released from cold surfaces.[6]

Many areas of the Earth's polar regions have long been considered to exist in a clean, almost pristine, state. However, in recent years, it has become increasingly apparent that this viewpoint is not entirely valid because, as well as acting as a sink for many chemicals, frozen land masses and cold airborne aerosols can also act as pollutant sources. For example, recent field measurements have shown the emission of both NO_x and HONO from the sunlit snowpack to be attributable to nitrate ion photolysis.[7−9] The observation is important because the role of nitrogen oxides in atmospheric chemistry cannot be understated as a result of their ability to generate tropospheric ozone, remove reactive OH radicals, produce NO_3 radicals, and play a role in VOC oxidation.

Various physicochemical processes are known to occur when a liquid sample is frozen, which can promote (electro)chemical reactions. A number of "freezing reactions" can be readily identified in this regard and may be categorized as type I, II, or III. Several clear differences exist between the categories. For example, types I and II take place in the liquid interfacial regions between ice crystals (often called "micropockets") within polycrystalline ice. By contrast, type III reactions occur on the surface of growing single ice crystals. Type I reactions simply involve the acceleration of a known solution-phase chemical reaction during freezing,[10−18] whereas type II processing requires an orientation effect during freezing to bring about new and unexpected chemical transformations.[19−21] Fundamentally, type III freezing reactions are of an electrochemical redox nature, with electron transfer taking place between the ice phase and the liquid (or liquid-like) layer on growing single-crystal ices.[22−24] The atmospherically relevant freezing reaction in the work reported here occurs in polycrystalline ice and is a type I reaction.

In this study, the production of nitric oxide (NO) and molecular iodine (I_2) from the freezing of two known sea-salt aerosol components, nitrite and iodide ions, has been investigated. The observations form the basis for the discovery of a previously unrecognized pathway involving the generation of labile gaseous compounds from frozen aqueous ionic species.

Experimental Section

Aqueous solutions of NO_2^-/I^- ions were frozen by two different methods. In method 1, the sample was frozen by placing the reaction vessel in a temperature-controlled ethanol bath cooled by a Neslab CC-100 Cryocool refrigerator unit, which was set at a fixed temperature of −23.2 °C. This setup allowed for analysis of both the gas phase and the solution phase. The gas phase was monitored in situ by a Monitor Europe NO_x chemiluminescence analyzer, while the ionic speciation of the solution phase was assayed before and after freezing using a HP8453 UV/vis diode array spectrophotometer. The experimental setup for method 1 is displayed in Figure 1. To prevent oxidation of the NO product, pure N_2 was used as a carrier gas to transport the gas-phase species to the NO_x chemiluminescence analyzer. The N_2 gas was maintained at a higher flow rate than the pump of the NO_x chemiluminescence analyzer so as to prevent air entering the system. One-half of the desiccator

* To whom correspondence should be addressed. E-mail: j.sodeau@ucc.ie.
[†] University College Cork.
[‡] Osaka Prefecture University.

10.1021/jp710464c CCC: $40.75

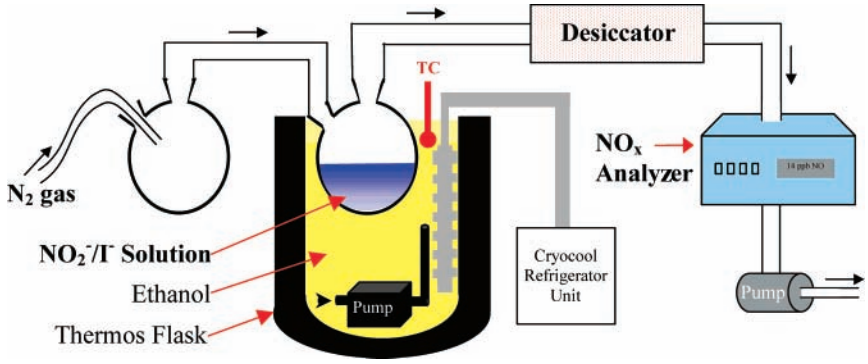

Figure 1. A schematic of the experimental setup for method 1. The thermocouple is marked TC. See text for more detail.

consisted of silica gel and the other half of phosphorus pentoxide powder (P_2O_5). The ethanol in the thermos flask was kept homogeneous by a pump immersed in the bath.

In method 2, the NO_2^-/I^- samples were placed in sealed polypropylene syringes in order to keep the dissolved oxygen concentration constant. The samples were subsequently frozen to −20 °C in a commercial freezer. Dissolved oxygen levels were not adjusted for the air-saturated experiments; however, for anoxic experiments, the dissolved oxygen content was reduced by bubbling N_2 gas through the solution. A WTW CellOx 325 oxygen sensor coupled to an Oxi 340 oximeter was utilized to measure the dissolved oxygen concentration. The nitrate ion was postulated to be a potential side product of the freezing reaction and, hence, was monitored by ion chromatography using a Dionex ICS1500 system (eluent: 12 mM Na_2CO_3; flow rate: 1.5 mL/min). For method 2, the ionic speciation of the solution phase was analyzed before and after freezing by use of UV/vis spectroscopy and ion chromatography; the gas phase was not monitored.

In both methods, the whole sample was frozen, that is, the temperature of the entire sample was below the freezing point of the solution in question. Instrumentation was not used to make this evaluation; it was simply determined by visual inspection. No acid was added to the systems to be frozen; however, the pH was recorded using a Horiba M-13 pH meter. Temperatures were measured using a Hanna Instruments 93531 thermometer with a type-K thermocouple.

Results and Discussion

The solution-phase, room-temperature reaction between nitrite and iodide ions has been studied in detail previously.[25−32] The overall reaction can be represented as

$$2HNO_2 + 2I^- + 2H^+ \rightarrow 2NO + I_2 + 2H_2O \qquad (1)$$

It has been shown previously that this process is so slow above pH 5.5 that it can be considered to be negligible,[32] and this result was confirmed in the current study. The generated I_2 combines rapidly with any iodide ions present in solution to form triiodide ions (I_3^-). Hence, the following equilibrium is set up

$$I_2 + I^- \rightleftharpoons I_3^- \qquad (2)$$

The equilibrium constant for eq 2 lies well to the trihalide side of the balance with values ranging from 698 to 714 L mol^{-1} [33−35] at 25.0 °C. Moreover, the forward reaction is an extremely fast, diffusion-controlled reaction with a rate coefficient of $k_2 = 5.6 \times 10^9$ M^{-1} s^{-1}.[36] The triiodide ion also possesses two strong distinctive absorption bands in the UV/vis region at 288 and 352 nm[37] with decadic molar absorption coefficients of 40 000 and 26 400 L mol^{-1} cm^{-1}, respectively.[34,38] All of the above factors make I_3^- an ideal proxy measure for the molecular iodine product in this system.

Hence, a 7.5 mM $NaNO_2$/KI solution with an initial pH = 6.10 was investigated as a function of freezing to −23.2 °C, as described in method 1. The production of triiodide ions after this solution has been frozen is clearly seen in the UV/vis spectrum displayed in Figure 2, following subtraction of the nitrite ion bands. Chemiluminescence monitoring allowed time profiles for gas-phase NO, NO_2, and NO_x released from the same thawing sample to be obtained. The result is shown in Figure 3, where arrow 1 marks the point at which the completely frozen sample was immersed in a hot water bath to initiate thawing and arrow 2 indicates the time at which the whole sample was completely thawed. Note that a slight inertia is present in the system due to the time taken for the gas to reach the analyzer. It can be clearly seen from the graph that NO is released from the sample to the gas phase during the thawing process.

Hence, from the above results, it can be concluded that acidifying a nitrite/iodide ion solution to pH < 5.5 is not necessary to cause release of molecular iodine and nitric oxide if the system undergoes a freeze−thaw process. The probability of such a freezing reaction occurring in the atmosphere is high, as a variety of natural freeze−thaw cycles are commonplace within, for example, cirrus clouds, snowpacks, freezing fog, hailstones, frost flowers, and glaciers. In fact, there is one known example published of such behavior occurring in the atmosphere, which involves the oxidation of nitrite to nitrate ions.[39] The potential structural driving forces in ices for such processes to occur are outlined below.

As stated above, type I and II polycrystalline freezing reactions occur in liquid micropockets between ice grains. These sites only exist within a certain temperature range between the freezing point and the eutectic temperature of the solution, which is known as the "frozen state".[40] At temperatures below the eutectic temperature, the liquid micropockets solidify, and the freezing reaction terminates.[40] For systematic investigations of these systems, it is therefore imperative to know the eutectic temperature of the multicomponent mixture in question. It is then necessary to perform the reaction above this temperature and below the freezing point of the solution. The eutectic temperature of the $NaNO_2-KI-H_2O$ three-component system has not been published, presumably due to its inherent complexity. However, the eutectic temperatures of the relevant binary systems are known, −26 °C for $NaNO_2-H_2O$[41] and −22.8 °C for $KI-H_2O$.[42] Furthermore, the eutectic temperature of any

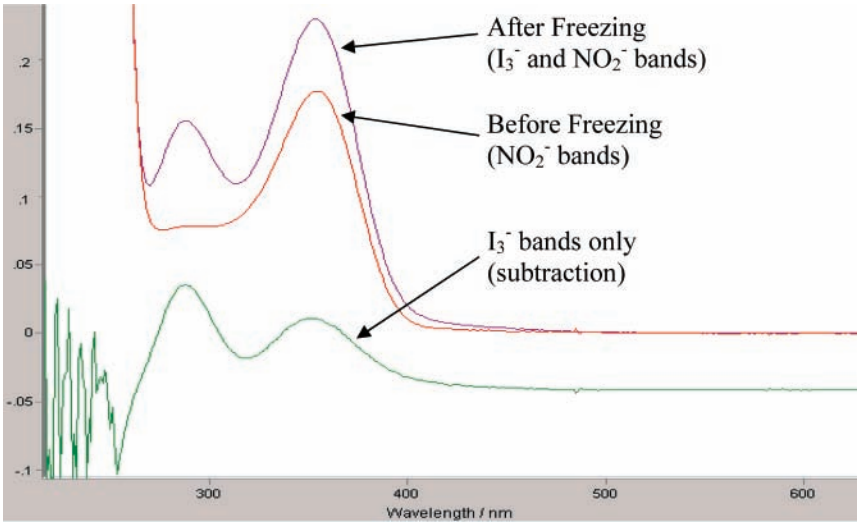

Figure 2. UV/vis spectrum of a 7.5 mM $NaNO_2$/KI solution before and after freezing. Initial pH = 6.10. Reaction temperature = −23.2 °C.

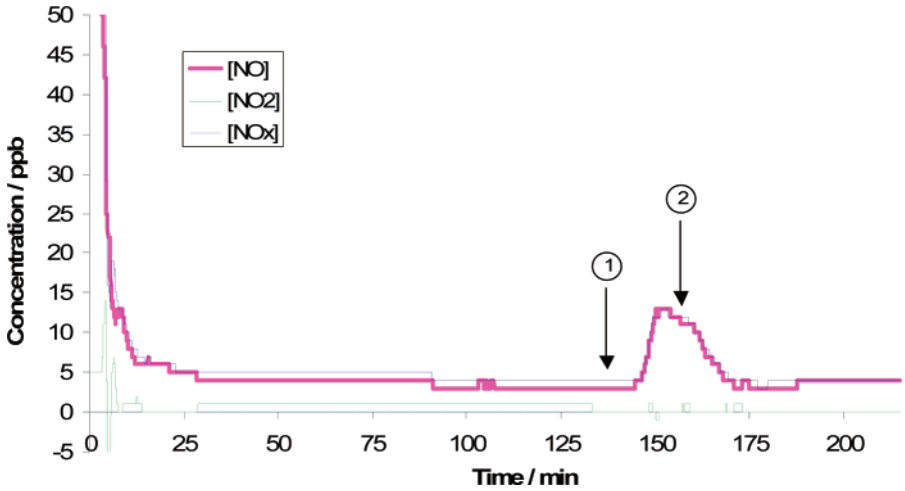

Figure 3. Time profile for NO, NO_2, and NO_x emitted from an aqueous 7.5 mM $NaNO_2$/KI solution during thawing. Initial pH = 6.10. Reaction temperature = −23.2 °C.

ternary system must be lower than its lowest binary eutectic temperature due to established phase-transformation laws.

A number of generic 3-D phase diagrams for ternary eutectic systems are published in the literature[43,44] and, hence, were used to visualize the various phases with decreasing temperature. If the ternary eutectic point was at a higher temperature than the lowest binary eutectic point, then a 2-D isothermal section of the 3-D ternary phase diagram would, at some stage, display a one-phase liquid region sharing a line boundary with a three-phase solid solution region. This feature would not conform with Gibbs's Phase Rule[45] or the "Law of Adjoining Phase Regions".[43,46−48] Hence, the eutectic temperature of any ternary system has to be lower than its lowest binary eutectic temperature.

This conclusion is supported by specific examples discussed in the literature[49] and by the definition of the eutectic point.[50−52] Therefore, the ternary eutectic temperature for the $NaNO_2$−KI−H_2O system would be found at a temperature lower than −26 °C, and a system of liquid micropockets would thus be expected to exist at the temperatures employed in the current study (i.e., −20 and −23.2 °C).

Liquid micropockets have been observed in both laboratory and field ice samples. For example, liquid regions between ice crystals in frozen laboratory samples have been detected by NMR spectroscopy[10,12] and microscopy.[53] Additionally, they have been observed in Antarctic ice samples by Raman spectroscopy,[54] scanning electron microscopy[55] and, in Antarctic and Greenland ice, by electrical conductivity methods.[56] The shape and geometry of the interfacial areas between ice grains are not well established but have been categorized into three main groupings, (a) lens-shaped inclusions (or films) at the grain boundaries between two ice grains, (b) triple junctions at the intersection of three ice grains, and (c) four-grain junctions at the point where four grain-boundaries meet, yielding a tetrahedron shape.[57] The junctions form at a variety of intersection points in the ice structure and thereby set up a three-dimensional network. The size of the interfacial areas (or micropockets) varies with temperature and solute concentration, as dictated by the phase diagram of the solution. Matsuoka et al. have used microscopy to measure the diameter of the lens-shaped inclusions in laboratory ice as 30−150 μm and the cross-sectional area of the triple junctions (in a frozen sample of 197 μM H_2SO_4 at −20 °C) to be about 10 μm^2.[53] Ice samples from Antarctica have been examined using scanning electron microscopy, and it has been found that the sulfur content is mainly located in an area of <1 μm^2 at the triple junctions (with

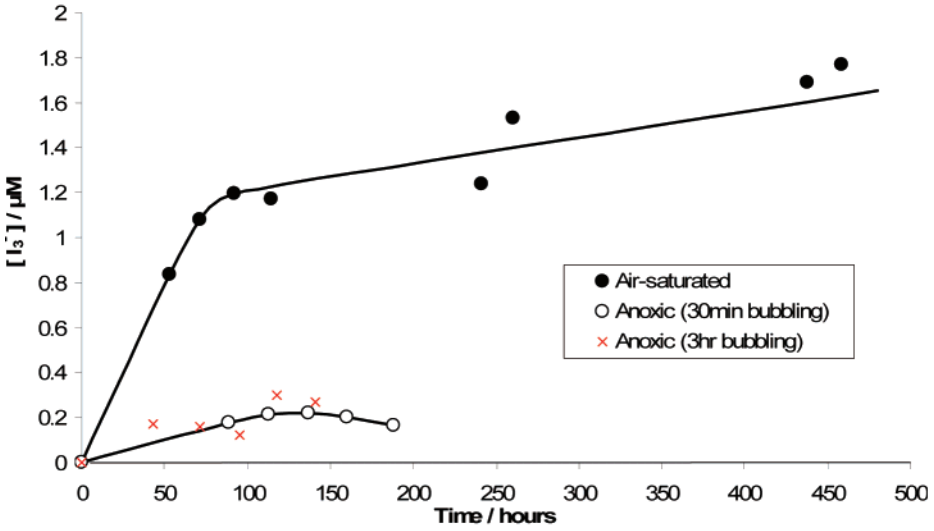

Figure 4. Graph of $[I_3^-]$ versus time for air-saturated and anoxic freezing experiments. Air-saturated (●): $[O_2]_0 = 7.45$ mg/L; Anoxic (30 min of N_2 bubbling) (○): $[O_2]_0 = 1.77$ mg/L; Anoxic (3 h of N_2 bubbling) (red ×): $[O_2]_0 = 0.93$ mg/L. $[NaNO_2]_0 = [NH_4I]_0 = 0.5$ mM. Initial pH = 5.79 ± 0.05. Reaction temperature = −20 °C.

concentrations greater than 1 M in the solid phase at −160 °C). In contrast, sulfur was undetectable in the bulk of the ice.[55] Ice from Nansen in Antarctica has been measured to have a triple junction cross-sectional area of 2 μm^2 at −20 °C, which decreases with temperature to <1 μm^2 below −35 °C.[54]

The acceleration of the NO_2^-/I^- freezing reaction in the current study has been mainly attributed to the well-known freeze−concentration effect. Ions rejected from the growing ice phase become concentrated in the liquid micropockets, as dictated by the solution's phase diagram. The increase in concentration in the micropockets results in an accelerated reaction with respect to its room-temperature counterpart, despite the lower temperature. The freeze−concentration effect has been observed in other freezing studies[10,12,14−17] and has been stated to be the main factor for the enhancement of freezing reactions.[20]

One of the fundamental differences between the polycrystalline freezing reactions (type I and II) is that the mechanisms of type I freezing reactions tend to follow that of their solution-phase counterparts, while type II reactions involve a previously unknown mechanistic pathway. However, there is some controversy in the literature regarding the exact nature of the reacting species in the solution-phase nitrite/iodide reaction at room temperature. The majority of the literature points toward the nitroacidium ion (H_2ONO^+) as the reacting species, which is formed by the fast pre-equilibrium step shown in eq 3[26−30]

$$HONO + H^+ \rightleftharpoons H_2ONO^+ \quad (3)$$

Kimura et al. seem to suggest that HONO is the reacting species, although the evidence used to support this conclusion is not definitive because of the presence of air in the reaction sample.[32] Therefore, all of the literature evidence points toward the involvement of a H_2ONO^+ reacting species. Subsequent reaction of this ion with iodide ions would form the intermediate nitrosyl iodide (INO) via the equilibrium shown in eq 4[29,30]

$$H_2ONO^+ + I^- \rightleftharpoons INO + H_2O \quad (4)$$

It has also been discovered that there are two parallel reaction pathways, path A, which is fourth order, and path B, which is sixth order.[29,30] Path A involves a slow reaction between the product INO and reactant I^- followed by a fast reaction with H_2ONO^+

$$INO + I^- \rightarrow NO + I_2^- \quad (5)$$

$$I_2^- + H_2ONO^+ \xrightarrow{\text{fast}} NO + I_2 + H_2O \quad (6)$$

Path B proceeds with the intermediacy of the ionic species, $H_2N_2O_3I^+$, as shown in eqs 7−9[29,30]

$$INO + HNO_2 \rightleftharpoons HN_2O_3I \quad (7)$$

$$HN_2O_3I + H^+ \rightleftharpoons H_2N_2O_3I^+ \quad (8)$$

$$H_2N_2O_3I^+ + I^- \rightarrow 2\,NO + I_2 + H_2O \quad (9)$$

In the cryosystem investigated in the current study, it might be expected that formation of H_2ONO^+ in the micropockets could be promoted by the well-known freeze−concentration effect. Hence, the small quantity of H^+ ions (or H_3O^+), initially present in the neutral solution (at pH 6.1) before freezing, becomes concentrated as water molecules are scavenged by the advancing ice front.[14] The "Workman and Reynolds" freezing potential of the system may also represent another factor that could enhance the formation of H_2ONO^+ by means of a proton-transfer mechanism across the ice−liquid interface.[58] Such changes in pH are commonplace in freezing reaction studies and have been well documented.[14,18,39,59]

Effect of Molecular Oxygen. As mentioned previously, it has been discovered that dissolved oxygen has a large influence on the solution-phase nitrite/iodide reaction at room temperature.[32] Hence, it was postulated to also have an effect on the nitrite/iodide freezing reaction. To investigate this hypothesis, eight air-saturated samples ($[O_2]_0 = 7.45$ mg/L), made up from the same stock solution of 0.5 mM $NaNO_2/NH_4I$ (pH = 5.79), were frozen to −20 °C in sealed polypropylene syringes held within a freezer, as described in method 2 above. Each sample was taken out at different intervals a day or two apart, thawed to room temperature, and analyzed. The results are shown in Figure 4. Analogous sets of experiments were carried out under anoxic conditions for the same concentrations of $NaNO_2$ and

TABLE 1: Calculation of the Total Number of Moles of I_3^- and NO after Freezing and the Ratio of I_3^- to NO

$[NO_2^-]$ and $[I^-]$	no. of moles I_3^-	no. of moles NO	ratio I_3^-/NO
7.5 mM	3.91×10^{-7}	3.86×10^{-9}	101.4
15 mM	5.71×10^{-7}	5.67×10^{-9}	100.6

NH_4I at a neutral pH. In one set, N_2 gas was bubbled through the solution for 30 min prior to freezing, which reduced the dissolved oxygen concentration to 1.77 mg/L. In a second set, the solution was purged for 3 h, which was shown to reduce the $[O_2]_0$ to 0.93 mg/L. These results are summarized in Figure 4, where it can be seen that the data points of the two anoxic experiments agree well. Hence, the reaction can proceed to a limited extent without oxygen, but it is also obvious that the concentration of dissolved oxygen has a large effect on the amount of product generated. Not only is there a higher concentration of triiodide ion produced in the presence of oxygen, but also, the shape of the resultant curve is different. This behavior can be rationalized by application of a chain reaction mechanism within the liquid micropockets of the ice structure, as discussed below.

Molecular oxygen trapped in the micropockets is capable of oxidizing nitric oxide to nitrogen dioxide (NO_2) in a termolecular process, as shown in eq 10

$$2NO + O_2 \rightarrow 2NO_2 \quad (10)$$

The product can then react in two ways, with I^-, as shown in eq 11, or with water, as shown in eq 12[31,32]

$$2NO_2 + 2I^- + 2H^+ \rightleftharpoons 2HNO_2 + I_2 \quad (11)$$

$$2NO_2 + H_2O \rightleftharpoons HNO_2 + H^+ + NO_3^- \quad (12)$$

Protonation of the nitrous acid produced by the above steps can form the nitroacidium ion (H_2ONO^+), as shown in eq 3. Therefore, the cycle would begin again, and a chain reaction mechanism would thereby become established. In fact, an increase in NO_3^- concentration during the freezing experiment was detected by ion chromatography, and hence, it can be concluded that the favored reaction pathway is via eq 12. The existence of this chain reaction mechanism is based on the likely assumption that the NO product cannot diffuse from the sample and, thus, is confined within the ice structure, leading to reaction with molecular oxygen. This feature indicates that the reaction occurs in the constraining environment of the liquid micropockets between ice grains.

In addition to the evidence presented in Figure 4, further proof exists of the chain reaction mechanism described above. The ratio of the number of moles of I_3^- to NO was calculated for the method 1 experiments, and the results are shown in Table 1. The number of moles of NO was calculated by integrating the NO peak in the time profiles, while the number of moles of I_3^- was calculated from the UV/vis spectra. It is clear from Table 1 that, for both experiments, the number of moles of I_3^- produced is about one hundred times the number of moles of NO produced. This ratio suggests that the NO is processed as described above to re-form the reacting species (H_2ONO^+), which, in turn, reacts with I^- to generate more I_2 and NO. Therefore, the number of moles of I_2 (and hence I_3^-) is enhanced in comparison to the number of moles of NO. (It is assumed that all iodine molecules are converted to triiodide ions as soon as they are formed). Considering that the stoichiometry of the reaction in eq 1 predicts the ratio of I_3^- to NO to be only about 0.5, a ratio of about 100 is very large and is further evidence for the presence of a chain reaction mechanism. This air-saturated NO_2^-/I^- freezing reaction, at pH 5.79 and −20 °C, has been estimated conservatively to be about 400 times faster than its solution-phase counterpart at room temperature.

Nitrite and iodide ions have been detected in different matrices throughout the atmosphere, for example, rain,[60,61] fog,[62,63] snow,[60,61] frost,[64] dew,[65] clouds,[66] marine aerosol,[67] ocean,[68−71] and brine waters.[72] Their concentrations in seawater range from sub-μM to μM levels,[68−71] making sea-salt aerosol a potential reaction site for the nitrite/iodide freezing reaction. At such concentrations, the freezing reaction has been estimated to cause sub-pptv increases in the NO mixing ratio in the surface layer (up to 100 m) of the atmosphere. This change is very small and would not significantly affect the measured NO levels of 2 pptv−2 ppbv.[73] However, the freezing reaction in this study only attained about 1% completion. Furthermore, the amount of NO released to the atmosphere would, of course, depend on the number of freeze−thaw cycles undertaken by the system, as shown in a previous study.[15] It is also known that additional inorganic salts can affect the extent to which freezing reactions proceed.[14] Hence, for all of the above reasons, it is difficult to quantify the exact atmospheric impact of the chemistry described in this study.

Conclusions

The freezing of ionic sea-salt components discussed above provides a previously unrecognized production pathway for the release of nitric oxide gas and iodine gas to the atmosphere. Moreover, the fact that the low pH values, required for the solution-phase reaction, can be readily circumvented by the presence of a freezing process creates a ready route to reaction under often-encountered cryospheric conditions. The nitrogen oxide gases play a critical role in the chemistry of the atmosphere, and therefore, any process that affects the NO_x budget needs to be examined in detail both in the laboratory and in the field. The importance of iodine in atmospheric chemistry has been demonstrated by its involvement in ozone-depleting processes in both the troposphere and stratosphere. In summary, this study demonstrates the potential influence of "freezing reactions" on the chemical balance of the cryosphere via the release of active, ozone-depleting gases and vapors to the air.

Acknowledgment. This research was generously supported by the Japan Society for the Promotion of Science (PE05009).

References and Notes

(1) Farman, J. C.; Gardiner, B. G.; Shanklin, J. D. *Nature* **1985**, *315*, 207−210.
(2) Solomon, S.; Garcia, R. R.; Rowland, F. S.; Wuebbles, D. J. *Nature* **1986**, *321*, 755−758.
(3) Bottenheim, J. W.; Gallant, A. G.; Brice, K. A. *Geophys. Res. Lett.* **1986**, *13*, 113−116.
(4) Oltmans, S. J.; Komhyr, W. D. *J. Geophys. Res.* **1986**, *91*, 5229−5236.
(5) Barrie, L. A.; Bottenheim, J. W.; Schnell, R. C.; Crutzen, P. J.; Rasmussen, R. A. *Nature* **1988**, *334*, 138−141.
(6) Simpson, W. R.; von Glasow, R.; Riedel, K.; Anderson, P.; Ariya, P.; Bottenheim, J.; Burrows, J.; Carpenter, L. J.; Friess, U.; Goodsite, M. E.; Heard, D.; Hutterli, M.; Jacobi, H. W.; Kaleschke, L.; Neff, B.; Plane, J.; Platt, U.; Richter, A.; Roscoe, H.; Sander, R.; Shepson, P.; Sodeau, J.; Steffen, A.; Wagner, T.; Wolff, E. *Atmos. Chem. Phys.* **2007**, *7*, 4375−4418.
(7) Honrath, R. E.; Peterson, M. C.; Guo, S.; Dibb, J. E.; Shepson, P. B.; Campbell, B. *Geophys. Res. Lett.* **1999**, *26*, 695−698.
(8) Beine, H. J.; Honrath, R. E.; Domine, F.; Simpson, W. R.; Fuentes, J. D. *J. Geophys. Res.* **2002**, *107*, 4584.
(9) Jones, A. E.; Weller, R.; Wolff, E. W.; Jacobi, H. W. *Geophys. Res. Lett.* **2000**, *27*, 345−348.

(10) Butler, A. R.; Bruice, T. C. *J. Am. Chem. Soc.* **1964**, *86*, 313−319.
(11) Eyal, Y.; Maydan, D.; Treinin, A. *Isr. J. Chem.* **1964**, *2*, 133−138.
(12) Pincock, R. E.; Kiovsky, T. E. *J. Am. Chem. Soc.* **1965**, *87*, 4100−4107.
(13) Takenaka, N.; Ueda, A.; Maeda, Y. *Nature* **1992**, *358*, 736−738.
(14) Takenaka, N.; Ueda, A.; Daimon, T.; Bandow, H.; Dohmaru, T.; Maeda, Y. *J. Phys. Chem.* **1996**, *100*, 13874−13884.
(15) Betterton, E. A.; Anderson, D. J. *J. Atmos. Chem.* **2001**, *40*, 171−189.
(16) Takenaka, N.; Furuya, S.; Sato, K.; Bandow, H.; Maeda, Y.; Furukawa, Y. *Int. J. Chem. Kinet.* **2003**, *35*, 198−205.
(17) Sato, K.; Furuya, S.; Takenaka, N.; Bandow, H.; Maeda, Y.; Furukawa, Y. *Bull. Chem. Soc. Jpn.* **2003**, *76*, 1139−1144.
(18) Takenaka, N.; Tanaka, M.; Okitsu, K.; Bandow, H. *J. Phys. Chem. A* **2006**, *110*, 10628−10632.
(19) Grant, N. H.; Clark, D. E.; Alburn, H. E. *J. Am. Chem. Soc.* **1961**, *83*, 4476−4477.
(20) Fennema, O. In *Water Relations of Foods*; Duckworth, R. G., Ed.; Academic Press: London, 1975; pp 539−556.
(21) O'Driscoll, P.; Lang, K.; Minogue, N.; Sodeau, J. *J. Phys. Chem. A* **2006**, *110*, 4615−4618.
(22) Finnegan, W. G.; Pitter, R. L.; Young, L. G. *Atmos. Environ.* **1991**, *25A*, 2531−2534.
(23) Finnegan, W. G.; Pitter, R. L. *J. Colloid Interface Sci.* **1997**, *189*, 322−327.
(24) Finnegan, W. G.; Pitter, R. L.; Hinsvark, B. A. *J. Colloid Interface Sci.* **2001**, *242*, 373−377.
(25) Bobtelsky, M.; Kaplan, D. *Z. Anorg. Allg. Chem.* **1930**, *189*, 234−240.
(26) Masek, J.; Przewlocka, H.; Vlcek, A. A. *Collect. Czech. Chem. Commun.* **1965**, *30*, 3594−3604.
(27) Ferranti, F.; Indelli, A.; Secco, F.; Lucarelli, M. G. *Gazz. Chim. Ital.* **1972**, *102*, 125−133.
(28) Dózsa, L.; Szilassy, I.; Beck, M. T. *Magy. Kem. Foly.* **1974**, *80*, 267−272.
(29) Dózsa, L.; Szilassy, I.; Beck, M. T. *Inorg. Chim. Acta* **1976**, *17*, 147−153.
(30) Ferranti, F.; Indelli, A. *Gazz. Chim. Ital.* **1980**, *110*, 273−277.
(31) Eguchi, W.; Tanigaki, M.; Mutoh, K.; Tsuchiya, H. *Kagaku Kogaku Ronbunshu* **1989**, *15*, 1109−1114.
(32) Kimura, M.; Sato, M.; Murase, T.; Tsukahara, K. *Bull. Chem. Soc. Jpn.* **1993**, *66*, 2900−2906.
(33) Palmer, D. A.; Ramette, R. W.; Mesmer, R. E. *J. Solution Chem.* **1984**, *13*, 673−683.
(34) Awtrey, A. D.; Connick, R. E. *J. Am. Chem. Soc.* **1951**, *73*, 1842−1843.
(35) Jones, G.; Kaplan, B. B. *J. Am. Chem. Soc.* **1928**, *50*, 1845−1864.
(36) Ruasse, M.-F.; Aubard, J.; Galland, B.; Adenier, A. *J. Phys. Chem.* **1986**, *90*, 4382−4388.
(37) Katzin, L. I. *J. Chem. Phys.* **1955**, *23*, 2055−2060.
(38) Meyerstein, D.; Treinin, A. *Trans. Faraday Soc.* **1963**, *59*, 1114−1120.
(39) Takenaka, N.; Daimon, T.; Ueda, A.; Sato, K.; Kitano, M.; Bandow, H.; Maeda, Y. *J. Atmos. Chem.* **1998**, *29*, 135−150.
(40) Pincock, R. E. *Acc. Chem. Res.* **1969**, *2*, 97−103.
(41) Helberg, M. H. *Ann. Chim.* **1925**, *10*, 121−125.
(42) Deluca, P.; Lachman, L. *J. Pharm. Sci.* **1965**, *54*, 1411−1415.
(43) Yeh, H. C. In *Phase Diagrams: Materials Science and Technology*; Alper, A. M., Ed.; Academic Press: New York, 1970; pp 167−197.
(44) Porter, D. A.; Easterling, K. E. *Phase Transformations in Metals and Alloys*; Van Nostrand Reinhold: New York, 1981.
(45) Gibbs, J. W. *Trans. Conn. Acad. Arts Sci.* **1875−1878**, *III*, 108−248; 343−524.
(46) Palatnik, L. S.; Landau, A. I. *Zh. Fiz. Khim.* **1955**, *29*, 1784−1803.
(47) Palatnik, L. S.; Landau, A. I. *Zh. Fiz. Khim.* **1955**, *29*, 2054−2073.
(48) Palatnik, L. S.; Landau, A. I. *Zh. Fiz. Khim.* **1956**, *30*, 2399−2411.
(49) Lide, D. R., Ed.; *CRC Handbook of Chemistry and Physics*, 85th ed.; CRC Press: Boca Raton, FL, 2005.
(50) Atkins, P. W. *Physical Chemistry*, 3rd ed.; Oxford University Press: Oxford, 1986.
(51) Welti-Chanes, J.; Bermúdez, D.; Valdez-Fragoso, A.; Mújica-Paz, H.; Alzamora, S. M. In *Handbook of Frozen Food*; Hui, Y. H., Cornillon, P., Guerrero Legarretta, I., Lim, M. H., Murrell, K. D., Nip, W.-K., Eds.; Marcel Dekker, Inc.: New York, 2004; pp 13−24.
(52) Sadoway, D. *Introduction to Solid State Chemistry: Phase Equilibria and Phase Diagrams*; MIT Open CourseWare: Cambridge, MA, 2004.
(53) Matsuoka, T.; Fujita, S.; Mae, S. *J. Phys. Chem. B* **1997**, *101*, 6219−6222.
(54) Fukazawa, H.; Sugiyama, K.; Mae, S. J.; Narita, H.; Hondoh, T. *Geophys. Res. Lett.* **1998**, *25*, 2845−2848.
(55) Mulvaney, R.; Wolff, E. W.; Oates, K. *Nature* **1988**, *331*, 247−249.
(56) Moore, J. C.; Wolff, E. W.; Clausen, H. B.; Hammer, C. U. *J. Geophys. Res.* **1992**, *97*, 1887−1896.
(57) Nye, J. F.; Frank, F. C. *Symposium on the Hydrology of Glaciers*; Cambridge, U.K., 1973; Vol. 95, pp 157−161.
(58) Workman, E. J.; Reynolds, S. E. *Phys. Rev.* **1950**, *78*, 254−259.
(59) Heger, D.; Klánová, J.; Klán, P. *J. Phys. Chem. B* **2006**, *110*, 1277−1287.
(60) Watanabe, N.; Kishi, M.; Hayakawa, O. *Yosui to Haisui* **1991**, *33*, 22−28.
(61) Gilfedder, B. S.; Petri, M.; Biester, H. *J. Geophys. Res.* **2007**, *112*, D07301.
(62) Miller, D. R.; Byrd, J. E.; Perona, M. J. *Water, Air, Soil Pollut.* **1991**, *32*, 329−340.
(63) Sigg, L.; Stumm, W.; Zobrist, J.; Zurcher, F. *Chimia* **1987**, *41*, 159−165.
(64) Mitchell, D. L.; Lamb, D. *J. Geophys. Res.* **1989**, *94*, 14831−14840.
(65) Okouchi, H.; Kajimoto, T.; Arai, Y.; Igawa, M. *Bull. Chem. Soc. Jpn.* **1996**, *69*, 3355−3365.
(66) Lammel, G.; Cape, J. N. *Chem. Soc. Rev.* **1996**, *25*, 361−369.
(67) Staebler, R.; Toom-Sauntry, D.; Barrie, L.; Langendörfer, U.; Lehrer, E.; Li, S.; Dryfhout-Clark, H. *J. Geophys. Res.* **1999**, *104*, 5515−5529.
(68) Orr, A. P. *J. Mar. Biol. Assoc.* **1926**, *14*, 55−61.
(69) Fukushi, K.; Nakayama, Y.; Tsujimoto, J. *J. Chromatogr. A* **2003**, *1005*, 197−205.
(70) Biswas, S.; Chowdhury, B.; Ray, B. C. *Talanta* **2004**, *64*, 308−312.
(71) Wong, G. T. F.; Zhang, L.-S. *Estuarine, Coastal Shelf Sci.* **2003**, *56*, 1093−1106.
(72) Amachi, S.; Muramatsu, Y.; Akiyama, Y.; Miyazaki, K.; Yoshiki, S.; Hanada, S.; Kamagata, Y.; Ban-nai, T.; Shinoyama, H.; Fujii, T. *Microb. Ecol.* **2005**, *49*, 547−557.
(73) Emmons, L. K.; Carroll, M. A.; Hauglustaine, D. A.; Brasseur, G. P.; Atherton, C.; Penner, J.; Sillman, S.; Levy, H.; Rohrer, F.; Wauben, W. M. F.; VanVelthoven, P. F. J.; Wang, Y.; Jacob, D.; Bakwin, P.; Dickerson, R.; Doddridge, B.; Gerbig, C.; Honrath, R.; Hübler, G.; Jaffe, D.; Kondo, Y.; Munger, J. W.; Torres, A.; VolzThomas, A. *Atmos. Environ.* **1997**, *31*, 1851−1904.